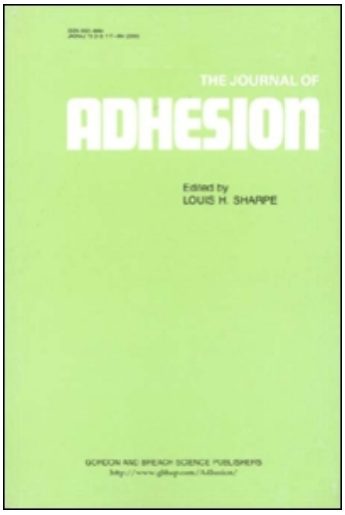

The Journal of Adhesion
Publication details, including instructions for authors and subscription information:
http://www.informaworld.com/smpp/title~content=t713453635

PARTICLE ADHESION AT THE NANOSCALE

K. Kendall[a]; C. W. Yong[b]; W. Smith[b]
[a] Chemical Engineering, Edgbaston, UK [b] CCLRC, Warrington, UK

Online publication date: 10 August 2010

To cite this Article Kendall, K. , Yong, C. W. and Smith, W.(2004) 'PARTICLE ADHESION AT THE NANOSCALE', The Journal of Adhesion, 80: 1, 21 — 36
To link to this Article: DOI: 10.1080/00218460490276731
URL: http://dx.doi.org/10.1080/00218460490276731

The Journal of Adhesion, 80: 21–36, 2004

ISSN: 0021-8464 print/1545-5823 online
DOI: 10.1080/00218460490276731

Taylor & Francis
Taylor & Francis Group

PARTICLE ADHESION AT THE NANOSCALE

K. Kendall
Chemical Engineering, University of Birmingham, Edgbaston, UK

C. W. Yong
W. Smith
CCLRC, Daresbury Laboratory, Warrington, UK

This article attempts to connect macroscopic observations of particle adhesion with the known interatomic forces which bind particulate interfaces together by studying contact between a plane surface and a sphere of smaller and smaller diameter. The fracture of a contact between a plane and a macroscopic sphere depends on the nonuniform stress distribution across the contact spot, causing atomic attraction at the edges of the contact region. Interface atoms some distance inside the contact region do not contribute to the adhesion. In fact, these inner atoms are in compression and are pushing the particles apart rather than causing adhesion. When a smaller sphere adheres to a plane at the nanoscale, this nonuniform stress distribution cannot be possible and the stress across the contact must be more even. To prove this hypothesis, molecular dynamics (MD) simulations have been carried out to study the fracture behaviour of subnano sodium chloride crystals. The MD models show clean fracture across the contact junction, in agreement with the macroscopic fracture studies. The models included explicit interatomic potentials to calculate the adhesion forces and contact stress distributions during particle pulloff as sodium chloride particles were altered in size. The results show that there is stress concentration at the contact edge for the smallest particles with 16 atoms (4 × 4) in contact.

Keywords: Particle adhesion; Molecular dynamics model; Fracture mechanics; Nanoparticles; Stress distribution; Sodium chloride

Received 28 July 2003; in final form 28 October 2003.

One of a collection of papers honoring Jacob Israelachvili, the recipient in February 2003 of *The Adhesion Society Award for Excellence in Adhesion Science, Sponsored by 3M*.

This research was carried out under a research grant from the EPSRC. The simulations were performed on the Daresbury Laboratory IBM/SP2 computer. The authors would like to thank the Editor, who brought Reference 8 to our attention.

Address correspondence to K. Kendall, Chemical Engineering, University of Birmingham, Edgbaston B15 2TT, UK. E-mail: k.kendall@bham.ac.uk

INTRODUCTION

Adhesion of molecularly smooth interfaces has been widely studied over the past decades, especially using graphite and mica, which can cleave and heal relatively reversibly over large areas, as demonstrated originally by Obreimoff [1]. Many years later, Tabor and Winterton [2] showed that the adhesion forces and jump to contact of mica surfaces could be explained by van der Waals forces. Then, Istraelachvili [3] demonstrated the surface chemistry of the interactions by showing the effects of liquid immersion, ionic contaminations, and the curious "stepwise jump to contact" observed in the presence of molecular adsorbed layers, which had to be squeezed out one by one as true atomic contact was approached.

Of course, Israelachvili used a macroscopic apparatus to make his measurements, based on Winterton's original design, in which cleaved mica sheets were glued to glass cylinders which could then be contacted to form a well-defined circular contact region about 1 mm in diameter. This atomic contact region was then studied by optical microscopy and interference techniques to determine the gap between the surfaces very precisely to within 0.1 nm. As the mica surfaces approached each other, they were assumed to be rigid up to the point of contact.

However, once adhesion forces are experienced, elastic deformations of the surfaces must occur, with the consequence that a nonuniform stress distribution is set up across the adhering contact spot [4]. Figure 1 shows how the contact stress distribution would be expected to vary with the length scale of the adhesion experiment. For macroscopic contact (Figure 1a) between an elastic sphere and a rigid flat (equivalent to crossed cylinders) the stress distribution is given by the JKR model [4], with a compressive stress at the centre of the contact and an "infinite" tensile stress at the edge of the contact spot, where fracture and healing occurs reversibly according to fracture mechanics. The atomic scale structure is not relevant to this model except for determining the value of the work of fracture, W, the single parameter which is determined by atomic properties in the JKR Equation (1):

$$d^3 = 6(1-\upsilon^2)D\{F + 6\pi WD/4 + [6\pi WDF/2 + (6\pi WD/4)^2]^{1/2}\}/E, \quad (1)$$

where d is the contact spot diameter, D the diameter of each equal crossed cylinder, F the applied compression force, υ is Poisson's ratio, and E is Young's modulus of elasticity.

By contract, for nanometer-scale contact between sphere and flat, the sphere is faceted and the flat is also atomically structured,

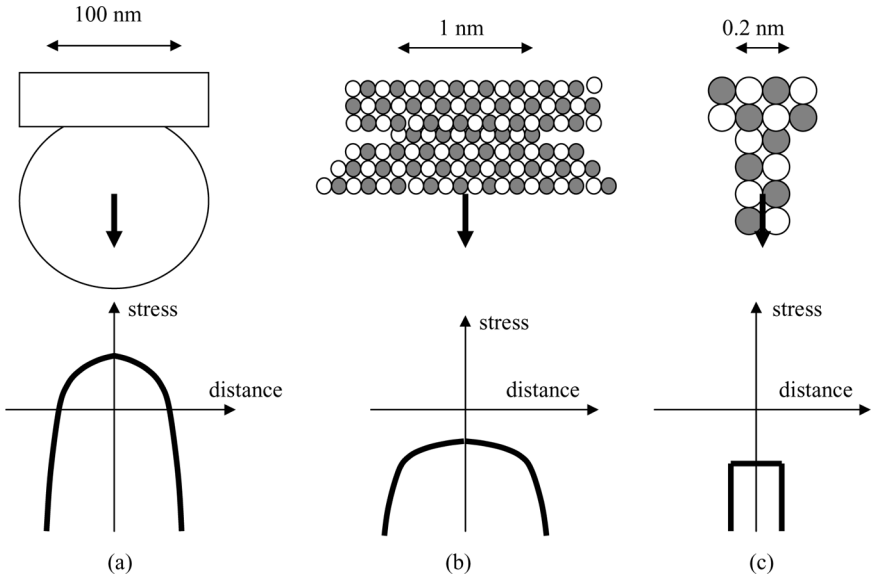

FIGURE 1 (a) JKR model of stress distribution for an adhering sphere to flat contact. (b) Realistic model of NaCl sphere/flat contact at the nm level. (c) Stress distribution for NaCl molecule adhesion.

as shown in Figure 1b. In this case we presume that the atoms meet in register and the there is no contamination. When a tensile force is applied to remove the sphere, the stress distribution is now on average very different from that of Figure 1a. The stress is near zero at the centre of the contact but is again "infinite" at the edges. Another problem with this atomic scale contact is that the range of influence of the interatomic forces can no longer be considered much smaller than the contact size, as in the JKR model. Consequently, we now need to insert at least two parameters into the adhesion model, one for the potential and the other for its range, as in typical molecular dynamics calculations [5].

As the contact is made smaller still, ultimately becoming two sodium chloride molecules in contact with the flat crystal, the time-averaged tensile stress can now only exist over the sodium and chloride ions and must essentially be constant as separation occurs. Of course, in this case the molecules are vibrating with thermal energy, and this effect must be modeled by molecular dynamics.

It is known that sodium chloride crystallites ($> 20\,\mu m$) tend to be brittle and crack easily [6]. Interestingly, our previous simulation

work [7] shows that retraction of small rectangular NaCl crystallites from commensurate (100) surface slabs also results in clean fracture, without leaving any material behind on the surface.

The purpose of this article is to extend our MD calculations in order to investigate the atomic adhesion and its transition to the macroscopic fracture by making comparison with the continuum mechanics model. Our aim is to investigate how and to what extent the continuum mechanics model fails (or holds) when discrete, atomic contacts are being considered.

Such a comparison has been attempted in the past. For instance, simple 2-D Lennard-Jones soft-disks have been used as the system models, and by changing the range of interaction, the work shows both ductile and brittle adhesional behavior of nanoparticles on surfaces [8]. In this work, we consider the atomic surface interaction behavior of crystalline NaCl in three dimensions using realistic interatomic interactions, with the Coulombic interaction being the dominant force.

MOLECULAR DYNAMICS MODEL

Sodium chloride was chosen for this study because it showed almost reversible, damage-free adhesion in previous calculations [7]. This was in contrast to magnesia [9, 10] and titania [7] models, which exhibited extensive plastic deformation and damage during the contact and removal process. The clean NaCl surface consists of a slab of (28×28) rows of NaCl lattice (Na-Cl distance of 0.279 nm) 6 layers deep. Periodic boundary conditions were applied parallel to the surface (xy direction) plane to mimic an infinite crystal surface with the (100) surface orientated at the z direction. To simulate discrete contacts, a small rectangular NaCl probe 6 layers thick was constructed, and this was varied in cross-section from (2×2) to (18×18) atoms to simulate increasing sizes of particle contact. Figure 2 shows part of the (2×2) atom probe model in section.

Detailed setup models and simulation procedures have already been described elsewhere [7] but will be described here briefly. The layers of NaCl atoms were classified into three different groups as shown in Figure 2. The first three layers of atoms (free) near the contacting surfaces, where commensurate contact was to take place, were allowed to move freely to reach their equilibrium positions. No constraint or adjustment has been introduced to these atoms, and this ensures that the natural outcome of the atomic configurations at the surface is entirely due to the interatomic interactions as mentioned below. However, atoms in the adjacent layers were coupled to the Berendsen heat bath [11] to maintain the temperature of the whole

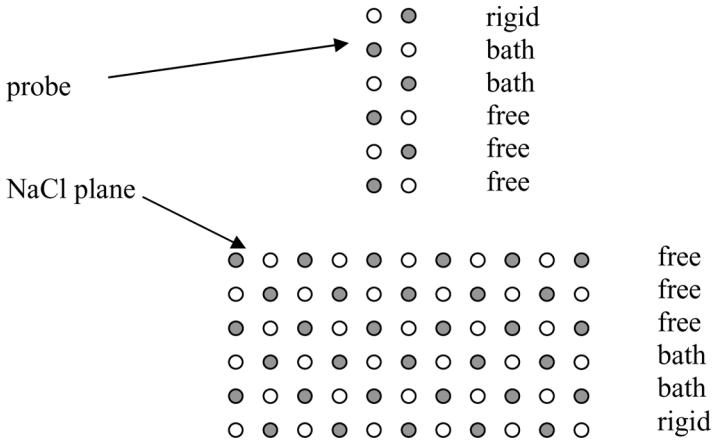

FIGURE 2 Schematic of the smallest NaCl probe approaching an NaCl surface.

system at 300 K; atoms (rigid) from the base surfaces were held fixed. The probe was arranged to make commensurate (100) contact with the NaCl plane surface. The initial gap was 0.7 nm where the van der Waal attractions were negligible. By moving the probe towards the plane, the attractive surface interaction profile with respect to surface distance can be obtained. The probe was then withdrawn to determine how fracture occurred at the atomic level. This is achieved as follows:

The DL_POLY [12] package was used to perform the MD calculations. All atomic interactions, V, were treated pairwise using the following potential functional form treating the atoms as rigid ions:

$$V(r) = Z_1 Z_2 e^2/r + A\exp[-r/\rho] - C/r^6, \tag{2}$$

where r is the interatomic distance, Z_1 and Z_2 are the charges of the atom pair, and e is the electron charge. The first term describes the long-range Coulombic electrostatic interactions. The second and third terms are the Buckingham potential that describes the short-range interactions. The second term is the core–core repulsive interaction. The third term is the attractive second neighbour van der Waals dispersion interaction. The parameters A, C, and ρ were empirically fitted to experimentally determined properties of NaCl such as elastic constants and crystal lattice parameters. Detailed potential fitting procedures and the parameter values for NaCl can be found in Catlow et al. [13].

The long-range electrostatic interactions were evaluated by 3D periodic Ewald summation [14] using the partial charge values of ± 0.988 for Na and Cl ions. Atomic trajectories were solved by the Verlet leap-frog algorithm [14] with a fixed time step of 0.5 fs. Initially, all movable atoms were assigned with initial velocities determined from a Gaussian distribution equivalent to a temperature of 300 K. The system was then allowed to equilibrate until a stable mean configurational energy was achieved, usually taking about 60–90 ps.

To make contact between the probe and the plane, the rigid layer of atoms in the probe was moved towards the surface over a successive integral distance of 0.005 nm, in the z direction. After each movement, the whole system was allowed to equilibrate for 2000 time steps (1 ps), followed by data sampling and averaging over a further 1000 time steps. This procedure is equivalent to a probe velocity of $3.33\,\mathrm{ms}^{-1}$ moving towards the NaCl crystal surface. The choice of equilibration periods ensured that after each probe advancement step, the whole system is in equilibrium before measurements were recorded. The response of the probe as a result of surface interactions was monitored by measuring the normal force, F_z, experienced by the rigid plane of the probe. This process was repeated from a large separation where there was no attraction (0.7 nm) to a point where large compression forces existed in the contact, so that a whole range of force profile with respect to distance between rigid planes of the surface slab and the probe, d_z, can be obtained.

CONTINUUM MECHANICS MODEL

The continuum model for adhesion in this situation is given by the diagram shown in Figure 3, which shows a rigid probe making adhesive contact with an elastic half-space. In Figure 3a, the rigid probe is assumed to be in perfect commensurate contact with the surface at the most stable configuration, that is, the probe experiences no loading. In this configuration, the tensile interactions are considered to be negligible.

As the pull-off force, F, is applied, the elastic substrate deforms into the shape shown in Figure 3b, with a tensile stress being developed at the contact junction. Subsequently, a crack initiates at the edge of the contact, diameter d, and moves through the interface to cause rapid fracture. The energy balance analysis was carried out [15] for this geometry by considering the three energy terms involved in the cracking:

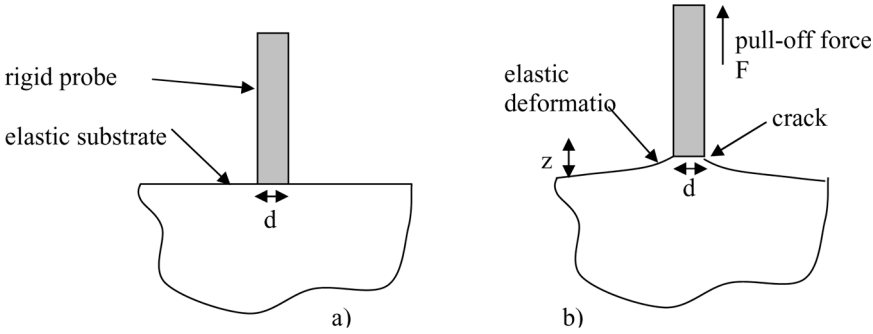

FIGURE 3 (a) A rigid probe making contact with an elastic surface. (b) Deformation of surface as pull-off force is applied.

1. Surface energy,

$$U_s = -W\pi d^2/4, \tag{3}$$

where W is the thermodynamic work of fracture, the energy required to break $1\,\mathrm{m}^2$ of interface reversibly.

2. Potential energy of the deflection, z, of a rigid punch diameter, d, in contact with an elastic substrate under load, F, was given by Boussinesq [5] in 1885:

$$z = (1 - v^2)F/Ed, \tag{4}$$

where E is Young's modulus and v is Poission's ratio.
Therefore the potential energy, U_p, is

$$-Fz = -(1 - v^2)F^2/Ed = U_p. \tag{5}$$

3. The elastic restoring energy, U_e, is half the potential energy and of opposite sign, that is,

$$U_e = -\frac{1}{2}U_p = (1 - v^2)F^2/2Ed. \tag{6}$$

Adding these three terms and applying the condition of energy conservation as the contact diameter, d, decreases,

$$\frac{d(U_s + U_p + U_e)}{dd} = 0. \tag{7}$$

Therefore,

$$F = \{\pi d^3 EW/(1 - v^2)\}^{1/2}. \quad (8)$$

The conclusion from this argument is that the adhesion force increases as the probe size is increased. But instead of the force going up with contact area, that is, d^2, it goes with $d^{3/2}$. In other words, the average stress (probe force/probe area) required for failure decreases for larger probes as $d^{-1/2}$. The adhesion stress, therefore, should increase for finer probes, but eventually must reach a limit as the probe reaches minimum atomic dimensions. The strength of this limit was calculated from the MD model as 4.0 GPa for a (2×2) atomic contact region (Table 1).

Obviously, the major difference between continuum and atomic length scales is the way the force is being handled. In the latter case, force contributions from discrete atomic interactions of the whole system have to be considered. Interestingly, as the results show in the following section, it turns out that rectangular blocks of NaCl making commensurate atomic contacts with the surface show interesting contact behaviour, similar to that of continuum mechanics prediction.

SIMULATION RESULTS

Figure 4 shows a typical F_z profile for NaCl surface interactions. For illustration purposes, the (8×8) probe is used as an example. Probes of other sizes were found to give similar qualitative results. Initially, as the probe was still far away from the surface, the interaction is negligible, with F_z registering a zero average. As d_z was decreased, a critical distance was reached whereby the probe was elongated and "jump to contact" with the surface (sharp change in F_z, towards negative

TABLE 1 Work of Fracture, W, and Average Adhesion Stress Calculated by Molecular Dynamics for Different Sizes of Contacts

Contact size	Area/nm^2	W/Jm^{-2}	Stress/GPa
(2×2)	0.3114	0.47	4.03
(4×4)	1.2455	0.48	3.06
(6×6)	2.8023	0.44	2.55
(8×8)	4.9818	0.45	2.42
(10×10)	7.7841	0.45	2.38
(14×14)	15.257	0.44	2.08
(18×18)	25.220	0.43	2.03

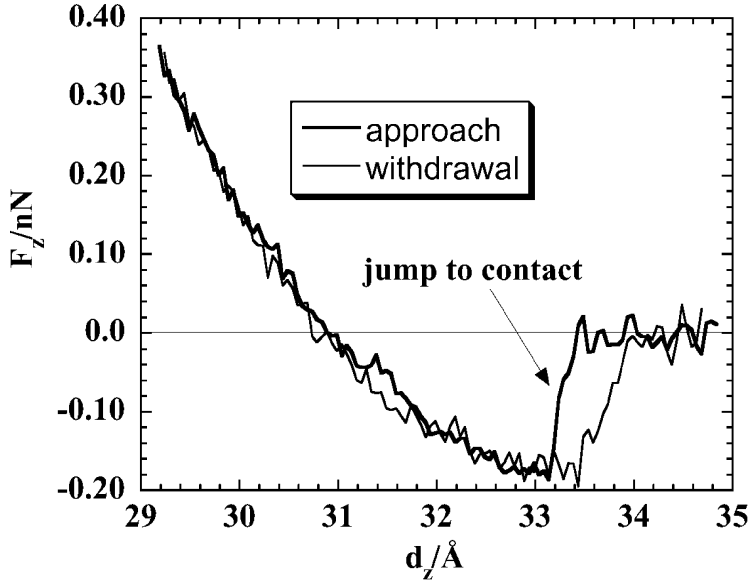

FIGURE 4 Force *versus* distance curves for the (8×8) probe interact with the surface slab. The bold line traces out the incoming process, and the thin line indicates the subsequent withdrawal process.

direction). As the distance was further decreased, the F_z gradually increased until the compressive force developed (positive F_z) as the probe was pressed against the surface. Subsequent probe withdrawal was essentially reversible, with the F_z profile following the same curve until the jump-to-contact region was reached, beyond which hysteresis occurred followed by a rapid increase of force, signifying a fracture. This was immediately followed by zero force averages as the probe was totally separated from the surface with no structural disruption to the probe.

In order to make qualitative comparison with the fracture Figure 5 shows an (8×8) probe at the jump to contact with the crystal surface under a tensile force. Note that the lines joining the atoms in the diagram can be used as a rough visual guide for the distances between ion pairs: a line is drawn between two atoms if the distance is close to or less than the equilibrium value; no line is drawn if the distance exceeds the equilibrium value. It is clear that the surface plane was deformed, with the surface atoms at the contact region raised and met with the probe, as expected from the continuum model. While Figure 5 is an instantaneous snapshot of the system, an analysis of a series of movie snapshots of the system trajectories showed that

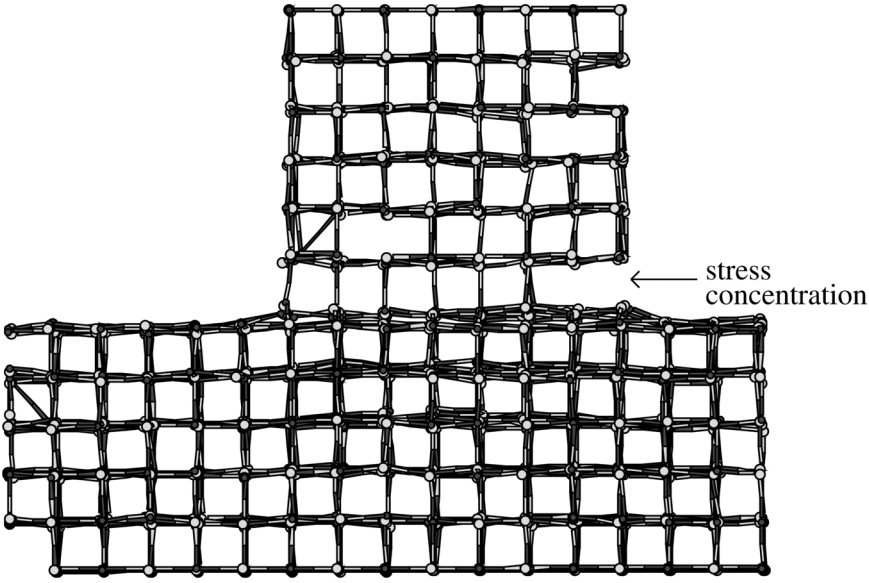

FIGURE 5 Atomic configuration of the (8×8) probe being pulled from the surface, showing the deformation near the contact region and the detachment starting at the edge of the contact (see Color Plate I).

detachment does start at the edge of the contact, in agreement with the continuum model. Furthermore, the average stress at pull off was calculated to be 2.42 GPa, which was significantly less than that for the (2×2) probe, as expected from fracture mechanics.

From Equation (8) it is assumed that d is the size of a contacting spot. In our MD models, the contacting planes are in fact squares of various sizes. Simulations for several probe sizes were carried out, and the result of maximum tensile forces versus $d^{3/2}$ is plotted in Figure 6. In this case, d is assumed to be the length of the rigid plane of the probe. Remarkably, the graph gives a straight-line relationship, indicating the fact that continuum mechanics still hold even at the atomic scales. The slope of the graph was determined without taking the smallest and largest probes into consideration. This is because the values of (2×2) probes are less reliable, due to large thermal fluctuation. Whereas, for the largest probe, (18×18), the force may be overestimated due to the fact that as the probe size increases, the rigidity of the probe also becomes significant, if the thickness remains unchanged. From Equation (6), the work of fracture can be determined, given that E and v for NaCl are 39.96 GPa and 0.252, respectively. In this way, the work of fracture is estimated to be $0.14\,\mathrm{Jm}^{-2}$.

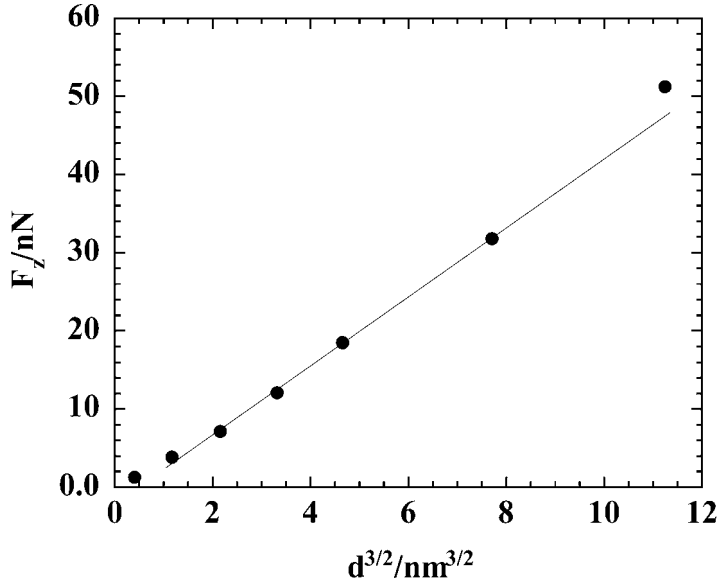

FIGURE 6 Maximum pull-off force *versus* probe size for NaCl. The straight line is the least-square fit for (4×4) to (14×14), inclusive.

The work of fracture can also be calculated from the model, that is, the difference in configurational energy between the system at its most stable state (the probe in contact with the surface at $F_z = 0.0\,\text{nN}$) and the system where the probe is far away from the surface divided by the probe area. The work of fracture together with the average stress at fracture, that is, the pull-off force divided by the contact area, are shown in Table 1 for different sizes of contacts. Once again, values for smaller and the largest probes are less reliable, due to the thermal fluctuations and model artifacts as mentioned above. The results show that for probes of increasing sizes, from (6×6) to (14×14), the work of fracture essentially remained constant, at about $0.45\,\text{Jm}^{-2}$, and the stress at fracture diminished. These trends are consistent with fracture mechanics predictions.

The calculated work of fracture is larger than that estimated from Equation (6). There may be two factors that cause discrepancy between the values: (1) the precise nature of contact junctions is less well defined where d is length of the approximately square planar contact, (2) The NaCl probes are a flexible, instead of a rigid, punch as is assumed in the continuum theory. These two factors may result in the work of fracture being underestimated from Equation (6). Nevertheless,

both values are in reasonable agreement, within a similar order of magnitude.

EXPERIMENTAL RESULTS

Experiments were conducted on melt-grown NaCl single crystals (BDH, London, UK) to measure fracture toughness and resistance to plastic deformation, as shown in Figure 7. A crack was initiated in the (100) plane of an NaCl crystal by pressing with a razor blade. This crack was then propagated controllably by applying a compressive force with a steel punch. From the continuum mechanics theory [16], the fracture toughness was calculated and is given in Figure 8. Similarly, by indenting the (100) crystal surface with a pyramidal punch, and dividing the applied force by the area of the indentation, the plastic yield stress of the NaCl was measured. NaCl is very anisotropic in its plasticity, yielding easily at around 2 MPa along (100) planes but requiring much larger stresses for displacement along (111) planes. The yield stress obtained from the indentation tests was 80 MPa.

From MD models, the fracture toughness is calculated to be $0.13\,\mathrm{MPa\,m^{1/2}}$, given that $W = 0.45\,\mathrm{Jm^{-2}}$. This is in good agreement with the experimental results. Of course, the toughness is found to increase with strain rate in the experiments. However, the MD models presumed a constant toughness at these low rates of deformation. This is because our system models are in equilibrium and the speed of probe movement is not relevant in our case.

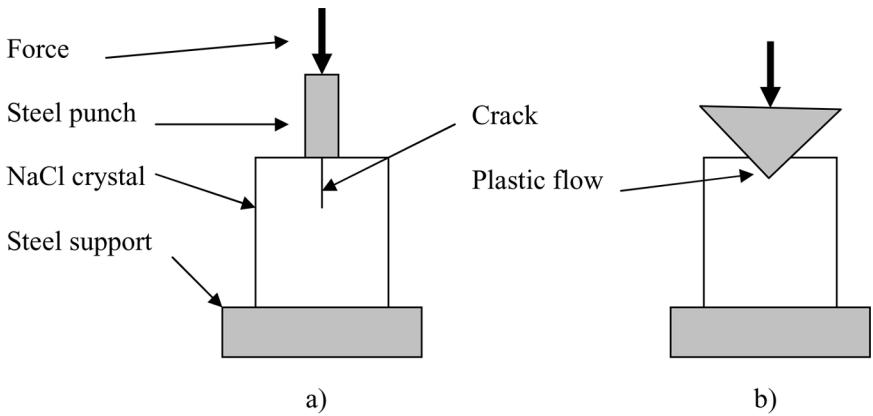

FIGURE 7 (a) Arrangement for determination of fracture toughness. (b) Vickers pyramid indentation test to measure plastic deformation of NaCl.

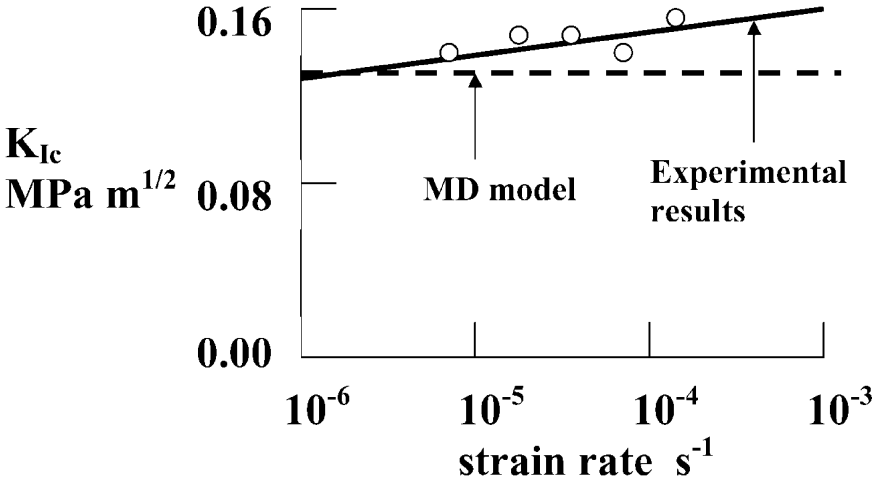

FIGURE 8 Fracture toughness of NaCl crystal along (100) planes.

DISCUSSION

The computational model has shown that the smallest NaCl probe adheres reversibly to the crystal surface with a maximum stress of about 4 GPa and a constant work of fracture of $0.45\,Jm^{-2}$. As the probe is made larger, the work of fracture remains constant but the stress at failure falls. These results highlight the fact that, for NaCl, descriptions of atomistic adhesive contact can be reasonably described by the continuum mechanics theory. Apparently, the faceted contact "spot" is still a reasonable approximation. However, the quantitative discrepancy arises due to the ill-defined nature of contacts, as well as the significance of flexibility of the contacting bodies at atomic scales.

In order to characterize the nature of the stress distribution just before fracture, Figure 9 shows the time-averaged atomic stress distribution of the middle section of the contacting plane for the (8×8) probe. The simulation results show that the stress distribution across the separation interface resembles that for large probes considered by fracture mechanics (Figure 1). High stress was observed at the edge of the contact with lower stress in the middle. The Boussinesq distribution for an elastic continuum is also included for comparison in Figure 9.

Although there was significant scatter in the average stresses computed for each atom, the statistical errors (derived from the coarse-graining block method [14] over a simulation time of 1 ns) were estimated to be in the order of ± 0.5 and the fit to the Boussinesq

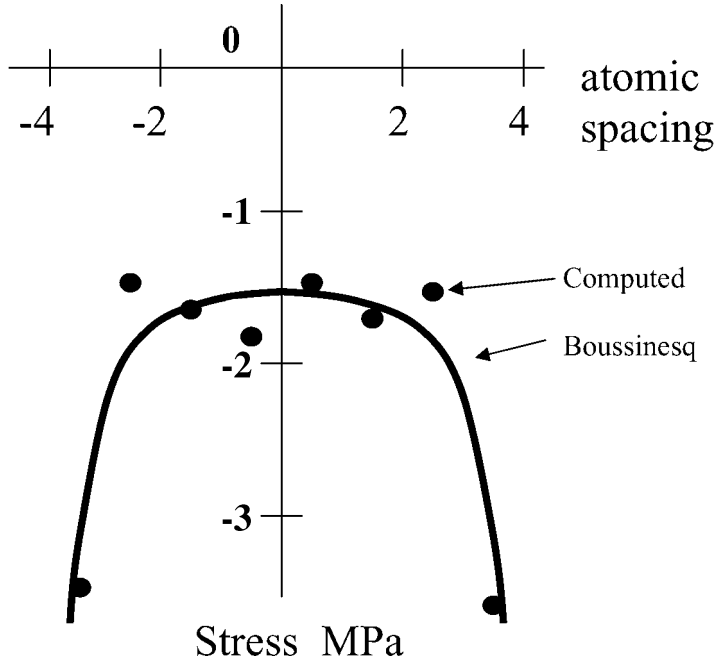

FIGURE 9 Computed tensile stress distribution across the middle section contact for an (8×8) contact for comparison with the Boussinesq continuum mechanics theory.

distribution was reasonable. This was not so for smaller contacts, below (4×4) atoms. The average stress at separation decreased for the larger probes, as expected from fracture mechanics theory, giving almost a $d^{-1/2}$ dependence for the smallest probes as shown in Figure 6 ($d^{3/2}$ dependence with respect to tensile force). Fracture mechanics seems to be operating even at the atomic scale.

The simulation work shows that probes of all sizes can be pulled off-with clean fractures at the contact junctions. There were no plastic deformations and no defects generated by the fracture process. This is in contrast to the experimental observations, whereby NaCl crystals can show considerable plasticity during fracture at 300 K. However, our work on MgO shows that detailed withdrawal behaviour depended very much upon the local geometry structure of the contacting planes. For a rectangular probe [9], the initial structural change occurred with defect creation in the middle of the probe, whereas for a step-pyramidal probe [10] this occurred near to the contacting tip. In both cases, subsequent pulling of these probes leads to plastic flows

and neck formations. However, our most recent work on NaCl shows that separating sodium chloride crystals can give either brittle or plastic behaviour, depending on the probe structure and the extent of probe compressions. These results will be published elsewhere in the near future.

CONCLUSIONS

The process of contact and fracture between NaCl probes and surfaces has been modeled by molecular dynamics for different contact dimensions, from (2×2) to (18×18). The smallest (2×2) contacts gave highly fluctuating stresses but a clear maximum separation stress of about 4 GPa. For larger contacts, the work of fracture remained constant, at $0.45\,\mathrm{Jm}^{-2}$, but the stress at failure decreased, indicating that fracture mechanics is operating even at the atomic level. Furthermore, the stress distribution is also in good agreement with the Boussinesq distribution, confirming the fact that, even at the atomic scales, fracture does occur at the edge of the contacting junction and propagates quickly towards the inner part of the junction.

The model became inaccurate above (14×14) contacts due to the inherent rigidity of the simulation models. No plasticity was observed in this perfect model, but the calculated fracture toughness is still close to the experimental observation. The simulation works also suggest that, for clean NaCl commensurate contacts, only small correction may be needed to the continuum mechanics descriptions in order to account for adhesion at the atomic scales. This includes introduction of the flexibility of the probe instead of treating it as a rigid body and better estimates for the highly facetted contacting plane.

REFERENCES

[1] Obreimoff, J. W., *Proc. Royal Soc. London* **A127**, 290–297 (1930).
[2] Tabor, D. and Winterton, R. H. S., *Proc. Royal Soc. London* **A312**, 435–450 (1969).
[3] Israelachvili, J. N., *Intermolecular and Surface Forces* (Academic Press, London, 1985), pp. 198–201.
[4] Johnson, K. L., Kendall, K., and Roberts, A. D., *Proc. Royal Soc. London* **A324**, 301–303 (1971).
[5] Kendall, K., *Molecular Adhesion and Its Applications* (Kluwer, New York, 2001), pp. 187–188.
[6] Roberts, R. J., Cowe, R. C., and Kendall, K., *Chem. Eng. Sci*. **44**, 1647–1651 (1989).
[7] Yong, C. W., Smith, W., and Kendall, K., *J. Mater. Chem*. **12**, 2807–2815 (2002).
[8] Quesnel, D. J., Rimai, D. S., and Demejo, L. P., *J. Adhesion* **67**, 235–257 (1998).
[9] Yong, C. W., Smith, W., and Kendall, K., *J. Mater. Chem*. **12**, 593–601 (2002).
[10] Yong, C. W., Smith W., and Kendall, K., *Nanotechnology* **14**, 829–839 (2003).

[11] Berendsen, H. J. C., Postma, J. P. M., van Gunsteren, W. F., DiNola, A., and Haak, J. R., *J. Chem. Phys*. **81**, 3684–3690 (1981).
[12] Smith, W. and Forester, T. R., *DL_POLY Version 2.12*, (CCLRC, Daresbury Laboratory, Warrington, UK.
[13] Catlow, C. R. A., Diller, K. M., and Norgett, M. J., *J. Phys. C* **10**, 1395–1412 (1977).
[14] Leach, A. R., *Molecular Modelling: Principles and Applications* (Longman, Singapore, 1996), pp. 302–306.
[15] Kendall, K., J. *Phys. D: Appl. Phys*. **4**, 1186–1195 (1971).
[16] Kendall, K., *Proc. Royal Soc. London* **A361**, 245–263 (1978).